Stratospheric ozone intrusion events, characterisation and distribution over high southern latitudes using ozonesondes.

Jesse Greenslade[1], Simon Alexander[2], Robyn Schofield[3,4], Jenny Fisher[1,5], and Andrew Klekociuk[2]

[1]*Center for Atmospheric Chemistry, University of Wollongong*
[2]*Australian Antarctic Division, Hobart*
[3]*School of Earth Sciences, University of Melbourne*
[4]*ARC Centre of Excellence for Climate System Science, University of New South Wales*
[5]*School of Earth & Environmental Sciences, University of Wollongong*

August 22, 2016

Abstract

We develop a quantitative method to identify Stratosphere to Troposphere Transport events (STTs) from ozonesonde profiles. Using this method we estimate the quantity of ozone transported across the tropopause over Melbourne (38°S), Macquarie Island (54°S), and Davis (69°S). STT seasonality is determined from a 7–9 year long time series of ozone profiles from each site. STT events primarily occur during summer above Melbourne and Macquarie Island, while there is little seasonal cycle in STT events above Davis. The majority of tropospheric ozone due to STT events occur within 3 km below the tropopause at Melbourne and Macquarie Island, and within 2 km below the tropopause at Davis. Overall, the fraction of total tropospheric ozone attributed to STT events is 2 – 4% at each site, however, during individual events, an STT event can contribute more than 10% of the total tropospheric ozone at that time. The GEOS-Chem model run with active stratospheric chemistry is too coarsely resolved in the vertical dimension to determine STTs. Simulated seasonal cycles of tropospheric ozone are well matched at all three sites although vertical profile averages have some bias in the troposphere. A conservative estimate of yearly tropospheric ozone flux due to STTs is calculated using the simulated tropospheric ozone column between 35°S and 75°S of 2.2×10^{16} molecules cm^{-2} yr^{-1} (TODO: update number once model finishes).

1 Introduction

Tropospheric ozone, which constitutes only 10% of the total ozone column, is an important oxidant, greenhouse gas and is toxic to biological life. Over the industrial period, increasing tropospheric ozone, has been estimated to exert a radiative forcing equivalent to a quarter of the CO_2 forcing [Forster et al., 2007]. Tropospheric ozone increases above pre-industrial levels are estimated to result in global losses up to $\$USD_{2000}$ 35 billion per annum until 2030 due to food crop impacts [Avnery et al., 2013] and up to $\$USD_{2000}$ 580 billion by 2050 (11.8 billion per year) due to health impacts [Selin et al., 2009]. Tropospheric ozone is produced anthropogenically by fossil fuel and biomass combustion emissions (NO_x and volatile organic compounds) that subsequently undergo photochemistry. Natural sources of tropospheric ozone include the downward transport from the ozone-rich stratosphere, wildfires and lightning photochemical production (Jacobson and Hansson [2000] and references therein).

Stratosphere to troposphere transport (STT) of ozone can increase regional surface ozone levels above air quality standard thresholds [Danielsen, 1968, Lefohn et al., 2011, Langford et al., 2012, Zhang et al., 2014]. A review of photochemical models by Stohl et al. [2003] (STACCATO) concluded that between 25-50% of tropospheric ozone can be attributed to SST events. A lower estimate was derived from the Atmospheric Chemistry and Climate Model Intercomparison Project (ACCMIP), [Stevenson et al., 2006] with 5100 ± 600 Tg/yr ($\sim 90\%$) and 550 ± 170 Tg/yr ($\sim 10\%$) of tropospheric ozone is due to chemical production and STT, respectively. Models are challenged to correctly represent STT, and process studies seem to be key in determining the relative role of SST in the tropospheric ozone budget.

STT events have been observed due to deep overshooting convection [Frey et al., 2015], tropical cyclones [Das et al., 2016] and mid-latitude synoptic scale disturbances (e.g. Stohl et al. [2003], Mihalikova et al. [2012]). STT events observed over the Mediterranian region estimate a 10% contribution to tropospheric ozone budget between 2000 and 2003 [Galani, 2003], with other observational studies noting significant occurrences and strong seasonal dependance (i.e. Lefohn et al. [2011]), contributing up to 30% of the surface ozone over the Western US in spring [Lin et al., 2012]. To date, while this topic has received significant attention in the tropics and northern hemisphere, observational estimates from the southern hemisphere extra-tropics is noticeably absent in the literature.

In the extra-tropics, ozone has a longer photochemical lifetime and STT events most commonly occur during synoptic-scale tropopause folds [Sprenger et al., 2003, Tang and Prather, 2012] which are characterised by tongues of high Potential Vorticity (PV) air descending to low altitudes. These tongues become elongated and filaments disperse away from the tongue and mix irreversibly into the troposphere. STT events have been observed in tropopause folds around both the polar-front jet [Vaughan et al., 1993, Beekmann et al., 1997], and the subtropical jet [Baray et al., 2000]. They are also observed near cut-off lows [Price and Vaughan, 1993, Wirth, 1995], which are often accompanied by

turbulent weather. A high correlation is found between lower stratospheric and tropospheric ozone [Terao et al., 2008] with the highest STT associated with jet-streams over the oceans in winter.

In section 2, nearly a decade of ozonesonde flight recordings from three locations spanning latitudes from 38°S - 69°S are used to characterise the seasonal cycle of STT events and determine their contribution to the total amount of tropospheric ozone. We examine the depth and frequency of the intrusions and use case studies to relate these STTs to meteorological events. Lastly, the fraction of total tropospheric column ozone attributable to STT events is calculated and an estimate of how much ozone this represents is made using a global chemical transport model.

2 Data and Methods

2.1 Ozonesonde record in the Southern Ocean

Ozonesondes are weather balloons with an attached instrument which measures ozone concentrations roughly every 100m from the surface to around 35km. These ozonesondes provide a high-vertical resolution profile of ozone, along with temperature, pressure, and humidity.

Ozonesondes use an electrochemical concentration cell which senses the proportional electrical current from ozone's reaction to a solution of potassium iodide. Each ozonesonde is completely new and independant, and only used once, and instrument calibration is not performed. Instead, standardised procedures are followed when constructing, transporting, and releasing the ozonesondes. Ozonesondes are estimated to provide around 2% precision in the stratosphere, which improves at lower altitudes [NOAA], although the accuracy has been shown to be around 5-10% which gets worse if standardised procedures aren't followed [Smit et al., 2007].

Ozonesondes are launched approximately weekly from Melbourne (38°S, 145°E), Macquarie Island (55°S, 159°E) and Davis (69°S, 78°E). For this study, we use the data collected from 2004-2013 for Melbourne and Macquarie, and 2006-2013 for Davis. Around twice as many ozonesonde launches occur at Davis prior to and during the ozone hole season (June-October) than at other times of the year [Alexander et al., 2013].

2.2 Characterisation of STT events and associated fluxes

Stratospheric ozone typically mixes irreversibly down (vertically) into the troposphere in kilometres-scale tongues of air. The strength (ozone enhancement above background levels), size, vertical depth, and longevity of these intruding ozone tongues vary due to weather, landscape, and season. While ozonesondes are released every week or so, ozone events may only be detectable for a matter of hours [Tang and Prather, 2012]. This makes the vertical ozone profile recorded by the ozonesonde highly dependent on the time of launch [Sprenger

et al., 2003], and we cannot guarantee that detected ozone enhancements are fully separated from the stratosphere.

In order to characterise tropospheric ozone events a clear definition of where the stratosphere begins is necessary. Two common tropopause height definitions are the standard lapse rate tropopause [WMO, 1957] and the ozone tropopause [Bethan et al., 1996]. The lapse rate is the negative altitudinal temperature gradient, and the lapse rate tropopause is defined as the lowest altitude where the lapse rate is below 2° C km^{-1}, provided the lapse rate between this altitude and all subsequent altitudes within 2 km is also below 2° C km^{-1}. The ozone tropopause is defined as the lowest altitude satisfying these three conditions [Bethan et al., 1996]:

1. Vertical gradient of ozone mixing ratio (OMR) is greater than 60 ppbv km^{-1}
2. OMR is greater than 80 ppbv
3. OMR between 500 m and 2000 m (1500 m in the Antarctic) above exceeds 110 ppbv.

At Davis, the ozone tropopause defintion is modified since the site is Antarctic and tropopause levels are lower near the poles. The ozone tropopause can be less robust during stratosphere-troposphere exchange, however it is more robust than the lapse rate tropopause at polar latitudes in winter and near jet streams in the lower stratosphere [Bethan et al., 1996, Tomikawa et al., 2009, Alexander et al., 2013]. In this work the lower of these two tropopause altitudes is used, as both are calculated for each ozonesonde release. This choice avoids occasional unrealistically high tropopause heights due to perturbed ozone or temperature measurements in the ozonesonde records.

Figure 1 shows the monthly mean tropopause altitudes at each location (solid lines). The mean tropopause altitude for ozonesondes which detected an STT is also shown (dashed lines). The seasonal cycle in tropopause altitude at Melbourne is exhibited, showing a maximum in summer, and a minimum is winter. This cycle is much more sublte at Macquarie, and almost reversed at Davis, which has a minimum during autumn and maximum from winter to spring. The decreasing tropopause altitude which occurs at higher southern latitudes is also apparent, as lower mean tropopause heights occur with more southern latitudes. The tropopause recorded by sonde is generally higher during an STT event at all three sites.

Figure 2 shows seasonally averaged ozone as recorded over the three stations. Increased ozone extending down through the stratosphere is apparent during December to March and September to November over Melbourne. These increased tropospheric ozone months are due to STTs (in summer), and possible fire smoke plume influence (in winter). Over Davis and Macquarie Island the tropospheric ozone is higher between March and October, although the effect is subtle compared to Melbourne.

Tang and Prather [2010] define one method of detecting these stratospheric tongues (or tropospheric ozone folds) as follows: From 5 km altitude, if the

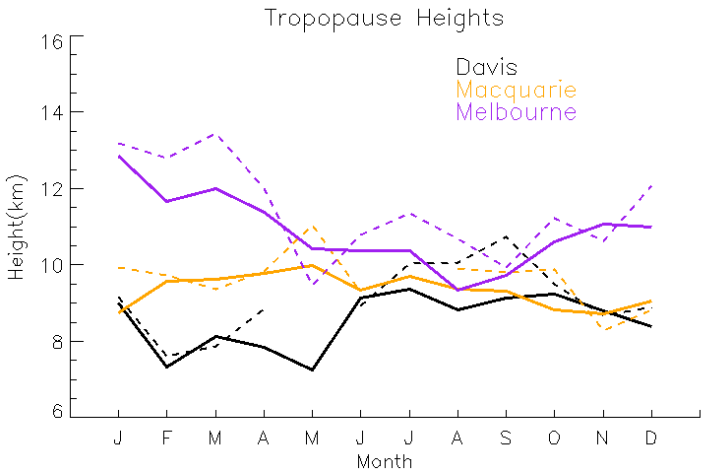

Figure 1: Monthly mean tropopause altitudes (minimum of lapse-rate and ozone defined tropopause at 3 sites) determined from ozonesondes. Dashed lines show the average monthly altitude when only considering dates when STTs occured.)

ozone level exceeds 80 ppb and then within 3 km decreases by 20 ppb or more to a value less than 120 ppb, then a tropopause fold has occurred. Their definition is based on subjective analysis of sondes released from 20 stations in the latitudinal range from 35°S to 40°N. We also characterise STT events using the ozonesondes vertical profiles, looking for tropospheric ozone enhancement above a local background (in moles per billion moles of air, or ppb). In this paper, tropospheric ozone events are characterised based on a subjective analysis of ozonesonde profiles at three sites at 38°S, 55°S, and 69°S. Part of the characterisation involves using a Fourier filter which removes high and low frequencies along the vertical dimension (the vertical scale), this filter is called a bandpass, since it retains a band of scales or frequencies.

To identify STT events, the vertical profiles of ozone volume mixing ratio are linearly interpolated to a regular grid with 20 m resolution up to 14 km altitude and are then bandpass filtered to retain perturbations with vertical scales between 0.5 km and 5 km. From here onwards the filtered vertical profile is referred to as the perturbation profile. The choice of band limits was set empirically; for an event to qualify as STT, a clear increase above the background ozone level is needed, and a vertical limit of $\sim$ 5 km removes seasonal-scale effects. We exclude from analysis perturbations at altitudes below 4 km above the surface to avoid surface pollution events and those occuring within 0.5 km of the tropopause to avoid the sharp transition to stratospheric air producing spurious false positives. Then using ozone perturbations from 2 km above the surface up to 1 km below the tropopause, we create a threshhold for each launch site at the 99th percentile. Profiles with perturbations exceeding this threshhold

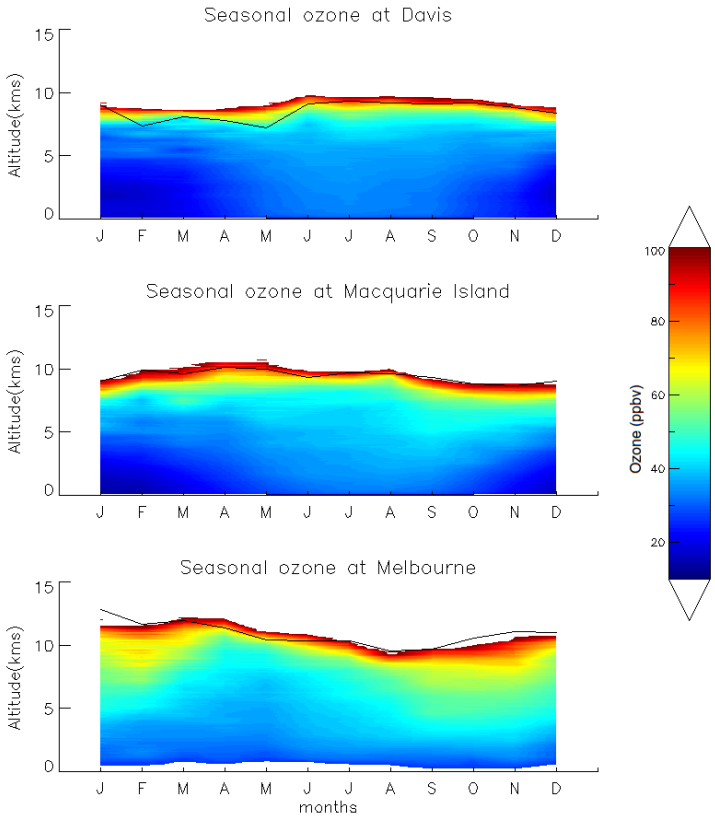

Figure 2: Seasonal cycle of ozone over Davis, Macquarie, and Melbourne measured by ozonesondes, where measurements are binned monthly. Black solid lines show seasonal tropopause heights, defined as described in the text.

are classified as STT events, subject to one more check.

The ozone peak is defined as the altitude where the OMR is greatest within the lowest range of altitudes where the perturbation profile exceeds the percentile based threshhold. If the OMR between this ozone peak and the tropopause drop below 80 ppb and are more than 20 ppb lower than the peak ozone then the event is confirmed, otherwise the profile is rejected as a non-event. This confirmation is only required if the perturbation profile does not drop below zero between the event peak and the tropopause. This happens in order to remove 'near tropopause' anomalies for which there is no evidence of detachment from the stratosphere.

We conservatively estimate the ozone flux into the troposphere associated with each event. The estimate is conservative since it does not take into any secondary ozone enhancements which may have been caused by the STT, as well as ignoring any heightened ozone background levels which may be due to synoptic-scale stratospheric mixing into the troposphere. The ozone flux calculation is made by integrating the ozone concentration enhancement vertically over the altitude range for which an STT event is identified. Figure 3 shows an example ozone profile, and how the algorithm detects an STT event, defines the event boundaries, and calculates the ozone flux.

2.3 Sensitivities and limitations

There are several observationally defined threshholds and limits which have an effect on how many events are detected, what altitude within which they can be detected, and how strongly the events are separated from the stratosphere.

The cutoff threshhold (defined locally to each site) is determined from the 99th percentile of the filtered ozone profile between 2 km and the tropopause height minus 1 kilometer. If an ozonesonde's filtered profile (between 4 km and the tropopause minus 500 m) goes above this threshhold then the profile is flagged as an event. Changing either of these altitude ranges, or the cutoff threshhold, changes how many events are detected. For example, using the 98.5th percentile increased detected events by 26 at Melbourne, 18 at Macquarie Island, and 9 at Davis. We use the 99th percentile because at this point the filter locates clear events with no obvious false positives.

The altitude range for flagging filtered profiles is set from 4 km above the surface to 500 m below the tropopause . This range removes possible ground pollution effects as well as local fire smoke plumes which are not likely to ascend above 4 km, as well as allowing event detection up to 500 m from the tropopause. Some events, including the storm-caused event examined in figure 5 are within one kilometer of the tropopause.

The altitude range used to determine the 99th percentile is set from 2 km up to 1 km below the tropopause. This range removes any anomalous edge effects of the Fourier bandpass filter, as well as discounting the highly variable ozone concentration which occurs near the tropopause.

TODO: Check and mention bandpass scale sensitivity.

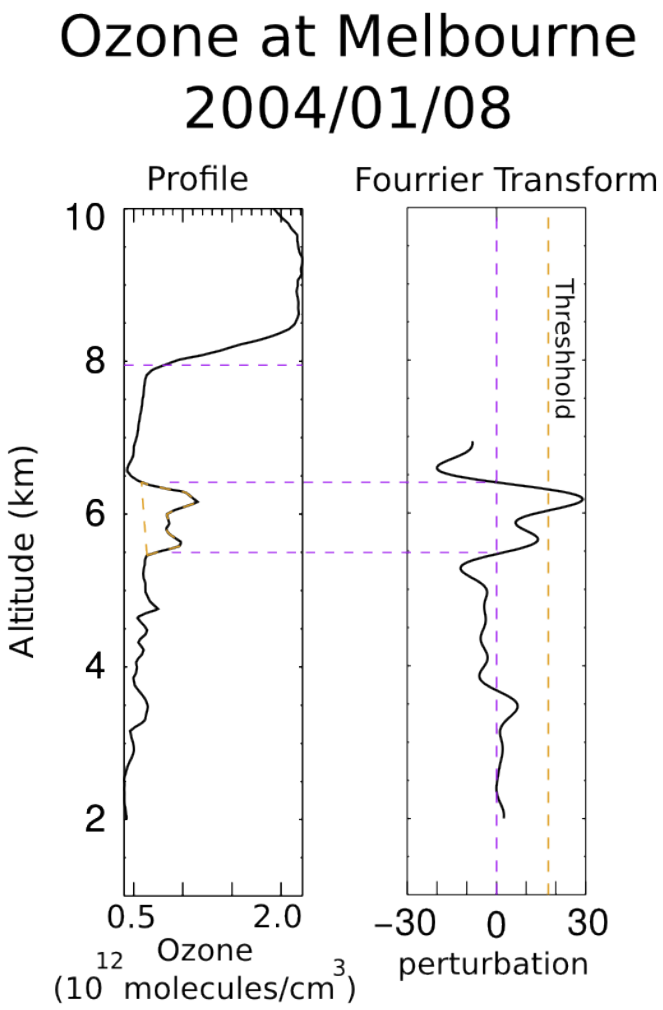

Figure 3: Left: an example illustrating methods used for STT identification and flux estimation using an ozone profile from 2km to the tropopause (dashed vertical line). At Melbourne on the 8th of January 2004, the flux area shows the estimate of stratospheric impact on tropospheric ozone. Right: bandpass filtered O_3 ppb perturbation profile. Coloured lines show the 99th percentile of filtered ozone perturbations (purple dashed) and the technique for determining the vertical extent of the event (orange dashed) is outlined in the text.

2.4 Removal of biomass burning influence

Other sources of tropospheric ozone profile perturbation need to be analysed and excluded before drawing any conclusions about STTs based on recorded ozone profiles. The major possible ozone influence other than STTs in the troposphere above 4 km is smoke plumes from biomass burning.

Ozone production from biomass burning is complex and affected by photochemistry, fuel nitrogen load, time since emission, and atmospheric plume chemistry both during transport and at the point of measurement. Large biomass burning events emit substantial ozone precursors, some of which are capable of being transported far from their origins. Peroxyacetyl Nitrate (PAN) is a reservoir of NO_x which can lead to enhanced ozone far from the source of a fire [Jaffe and Wigder, 2012].

Biomass burning influence in the Southern Hemisphere comes mostly from Southern Africa and South America, however Australian fires from the mid-latitudes, and Indonesian fires can also influence the ozonesonde release sites. Transported biomass burning plumes influence the southern mid-latitudes generally between July and December [Pak et al., 2003]. Biomass burning smoke plumes can lead to enhanced ozone, however this is not always the case. Due to the chance of smoke plume influence on STT characterisation, events which occur near smoke plumes are flagged and not included in STT flux calculations.

Removal of any possible influence from biomass burning smoke plumes is performed by detection of smoke plumes through global CO measurements. Here we identify transported smoke plumes through enhanced carbon monoxide (CO) levels. CO has a long enough lifetime to be an effective tracer of transport. The primary source of atmospheric enhancement of CO is fires, making CO a good indicator of fire plumes. Using high CO levels as a proxy for smoke plumes is a well established method (eg: Edwards [2003], Sinha et al. [2004], Edwards et al. [2006], Mari et al. [2008]). We use data from the AIRS (Atmospheric Infrared Sounder) instrument on board the Aqua satellite [AIR, 2013]. A visual inspection of AIRS' vertical columns of CO over the Southern Hemisphere is performed in order to exclude events with possible smoke influence at our three sites. We diagnose smoke plumes where high ($\sim 2 \times 10^{18}$ molecules cm^{-2} or higher) CO columns appear and when these occur near our sites during a sonde-detected ozone event, the event is flagged.

Figure 4(top) shows a day where smoke plumes are near the Melbourne sonde launch site on the day of a detected event. An event preliminarily detected on this day through the ozonesonde data is flagged as possibly due to fire. In the figure elevated CO levels can be seen over Australia, likely due to long-range transport from African and/or South American biomass burning. This day can be contrasted with the example in figure 4(bottom) where low CO levels are observed over the entire Southern Hemisphere. We screened all days at all three sites where an STT event is detected except for one event that coincided with missing AIRS data (January 2010). We flagged 15 of 72 events over Melbourne, 8 of 48 events over Macquarie island, and none from 45 over Davis. Nearly all of the discarded events occur within the burning season of the Southern

Hemisphere.

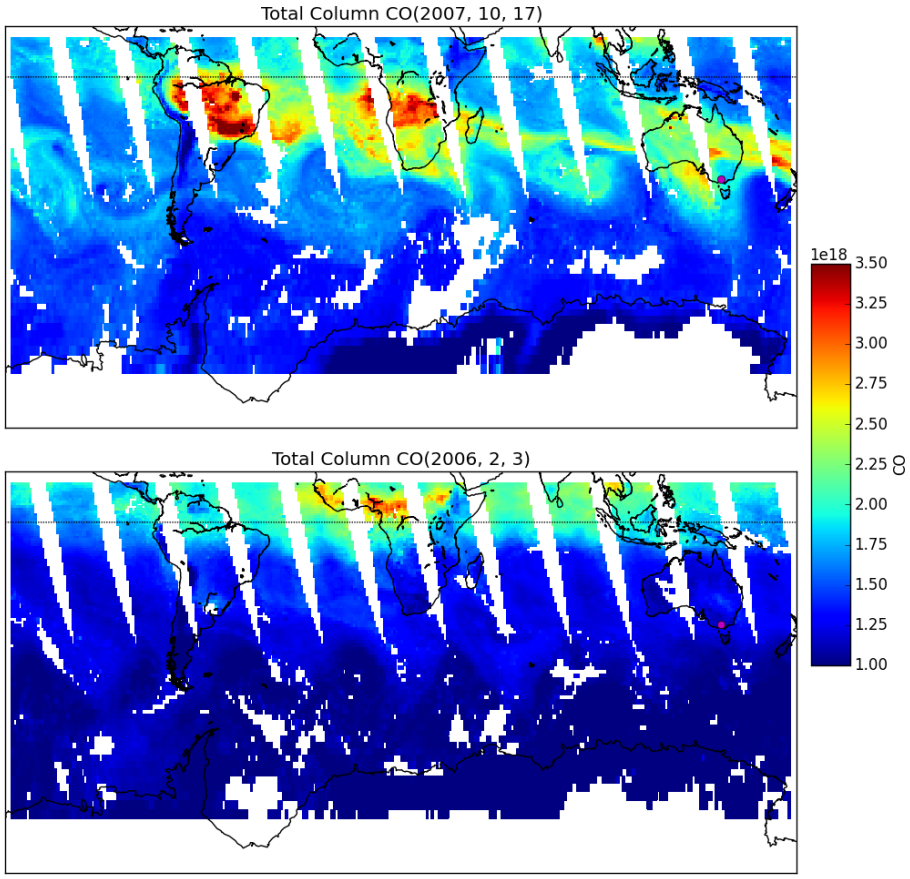

Figure 4: AIRS total column CO. The top panel (17 October 2007) is a day when ozone above Melbourne (purple dot) could have been caused by a transported biomass burning plume, and so was excluded from analysis. The bottom panel (3 February 2006) shows an example of a day when Melbourne ozone was likely not influenced by transported smoke plumes and was retained for analysis.

STT events flagged in this way are included in Figures 7 to 9, they are coloured red and do not contribute to STT flux calculations. These flagged events are concentrated in spring at Melbourne and Macquarie Island, and don't have any otherwise notable characteristics.

3 Case Studies of synoptic conditions during STT events

We examine two case studies in detail to illustrate the synoptic-scale conditions in which STT events occur over Melbourne. Data from the European Center for Medium-range Weather Forecasts (ECMWF) Interim Reanalysis (ERA-I) [Dee et al., 2011] product is used for synoptic-scale examination of weather patterns over our three sites on dates matching detected STT events.

Figure 5(left) shows the ozonesonde profile recorded on the 3rd of February 2005 above Melbourne. Both tropopause definitions are between 400 and 500 hPa and the ozone spikes have clear anticorrelations with the relative humidity, suggesting dry stratospheric air is measured here. An ozone intrusion into the troposphere is identified by our detection algorithm at $\sim$ 520 hPa. Figure 5(right) shows the synoptic weather system, a cut-off low pressure system which caused a large storm and lowered the local tropopause height for several days. The wind circles around the low pressure system in a clockwise direction, typical geostrophic flows which are caused by pressure gradients and coriolis forces. The flux of stratospheric ozone brought into the troposphere by this event is at least 3.1×10^{11} molecules cm^{-3} , or 8% of the tropospheric ozone column.

Figure 6(left) shows the vertical ozonesonde profile recorded on the 13th January 2010 over Melbourne. The tropopause heights are greater at this time and an ozone intrusion is identified centred around 200 hPa. Again, anticorrelated relative humidity provides evidence that the air is stratospheric in origin. Note the separation between this intrusion and the ozone tropopause (marked by the black dashed line), which indicates that the sonde passes through regular tropospheric air after hitting a stratospheric intrusion but before reaching the tropopause. Figure 6(right) shows a trough of low pressure (a low pressure front) passing over south-eastern Australia. This low pressure system crosses west to east and causes a wave of lowered tropopause height, which is often the cause of stratospheric mixing. During frontal passage, stratospheric air descends and streamers of ozone-rich air break off and mix into the troposphere [Sprenger et al., 2003].

An investigation of the ERA-I synoptic weather during STT events above Melbourne, Macquarie Island, and Davis are performed and are used to subjectively classify the events based on their likely cause. Similar characteristics to the case studies presented here occur over Macquarie Island: i.e. a prevalence of frontal and low pressure activity during STT events. Typically during STT occurrence, the upper troposphere is not calm, with low pressure fronts or cut-offs nearby at coincident time. Over Davis the weather systems are harder to distinguish, and the polar vortex may create ozone folds without other sources of upper tropospheric turbulence.

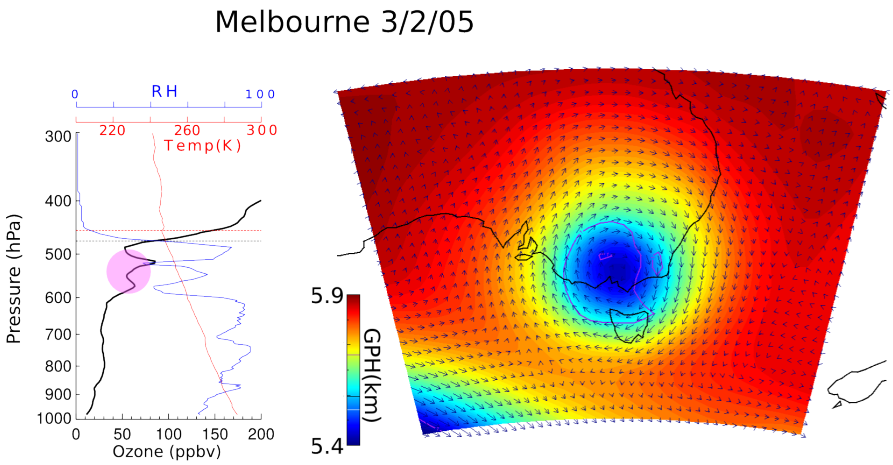

Figure 5: (Left) Vertical profile of ozone (black line), relative humidity (blue line), and temperature (red line) for 3 February 2005. The STT ozone event is highlighted in pink. The tropopause heights using both the ozone definition (black dashed line) and lapse rate definition (red dashed line) are shown. (Right) Synoptic weather map at 500 hPa from the ERA-Interim reanalysis. Vectors show wind direction and speed while colour indicates the geopotential height. Also visible are contours of potential vorticity units with 1 PVU in purple.

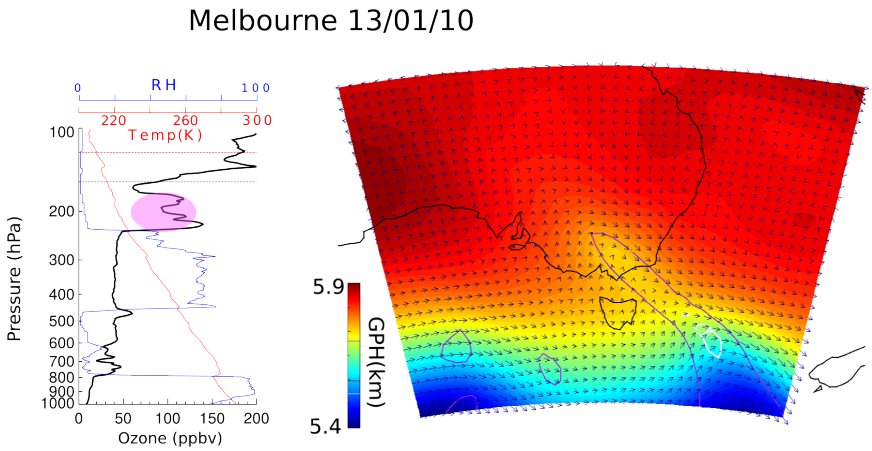

Figure 6: As figure 5, for 13 January 2010. Additionally visible is a 2 PVU contour, often used to determine dynamical tropopause height, in white.

4 STT event climatologies

Figure 7 shows the seasonal cycles of the STT events for Melbourne, Macquarie Island, and Davis. There is an annual cycle with a summertime peak in the frequency of STT events above Melbourne and Macquarie Island. This summertime peak is due to a prevalence of summer storms, with low pressure systems bringing storms and turbulence along with a lowered tropopause level [Reutter et al., 2015].

A subjective analysis of ERA-I synoptic scale wind and altitude at 500 hPa over the three sites (eg: figure 5(right)) leads to the categorisation of events based on their probable climatological cause. Probable causes are either low pressure fronts, low pressure cutoffs, or undetermined(misc). These categories are coloured as shades of blue in plots 7-9. This analysis suggests that low pressure cut off systems are more prevalent in late summer at both Macquarie and Melbourne, and during winter at Davis.

The frequency of STT events above Davis is relatively constant throughout the year, with a slight increase in events during antarctic winter. The slightly increased winter time frequency can be attributed to the increased frequency of sonde releases during the June to October months over Davis. It could be that events are non seasonal at Davis, or else that the sample of 45 detected events over 10 years is too small or sparse to clearly show any cycle. It is possible that summer events caused by upper troposphere turbulence are balanced out by the events caused by the polar front jet stream, which is strongest during antarctic winter. The polar front jet stream is a band of wind extending from the mid

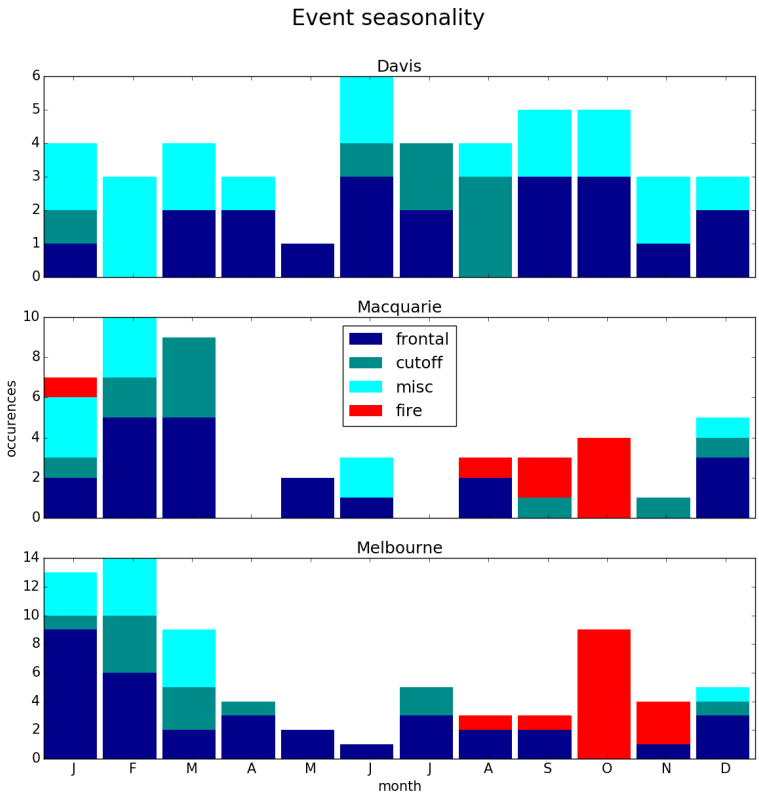

Figure 7: The seasonality of STT events at Davis, Macquarie Island, and Melbourne. Events are categorised by associated weather, and coloured bars from each category are stacked atop one another. The events filtered out as possibly smoke plume influenced are displayed here in red.

troposphere up to the lower stratosphere, which is generally active from winter to spring. This vortex may be directly causing or impacting many of the STTs due to the lowered tropopause altitude which occurs south of the vortex edge (around 60°S).

Figure 8 shows the altitudes of detected events, based on the peak (maximum) of tropospheric ozone. STT event peaks most commonly occur at 6 – 10 km above Melbourne and below 8 km at Davis but are distributed more evenly at Macquarie Island, up to 7.5 kilometres altitude. Figure 9 shows the depths of detected events, based on the ozone peak's distance from the minimal determined tropopause. The majority of event peaks occur within 3 km of the tropopause at both Melbourne and Macquarie Island, and within 2 km of the tropopause at Davis.

For both Melbourne and Macquarie Island, the STT events which are unlikely to be fire-related occur mostly in summer and mostly during low pressure synoptic systems which can increase convection and upper tropospheric turbulence.

5 Comparison with GEOS-Chem

GEOS-Chem is a global chemical transport model [Bey et al., 2001], which includes transport, emission, deposition, chemical production and destruction of ozone and 103 other trace gases throughout the troposphere along with stratospheric chemistry, including photolysis. Stratosphere-troposphere coupling is calculated using the stratospheric unified chemistry extension (UCX) [Eastham et al., 2014], which includes a further 28 trace gases. For comparison to ozonesonde observations, we use GEOS-Chem version 10-011 (including UCX) run from 2005-2012, following a 1-year spin-up for 2004. Transport is driven by assimilated meteorological fields from the Goddard Earth Observing System (GEOS-5) maintained by the Global Modeling and Assimilation Office (GMAO) at NASA. Our simulation was modified from the standard v10-01 to a fix a bug in the treatment of the Total Ozone Mapping Spectrometer (TOMS) satellite data used to calculate photolysis (see Henderson [2016]). The simulation uses 2° latitude by 2.5° longitude horizontal resolution, with 72 vertical levels from the surface to 0.1 hPa. Biogenic emissions of organic chemicals are determined by the Model of Emissions of Gases and Aerosols from Nature (MEGAN) version 2.1 extended by Guenther et al [Guenther et al., 2012]. Anthropogenic emissions are given by the Emissions Database for Global Atmospheric Research (EDGAR) version 4.2.

Ozonesondes are useful for looking at specific locations with high resolution, and in this work they provide an estimate of both STT occurence rates and STT ozone flux. This information can be used in conjunction with global scale information in order to extrapolate ozone transport over a large area. GEOS-Chem is used to simulate the global ozone concentrations. In order to check that the model is reasonable, some simple validation is performed. Comparisons of both ozonesonde and GEOS-Chem simulated tropospheric ozone profiles and

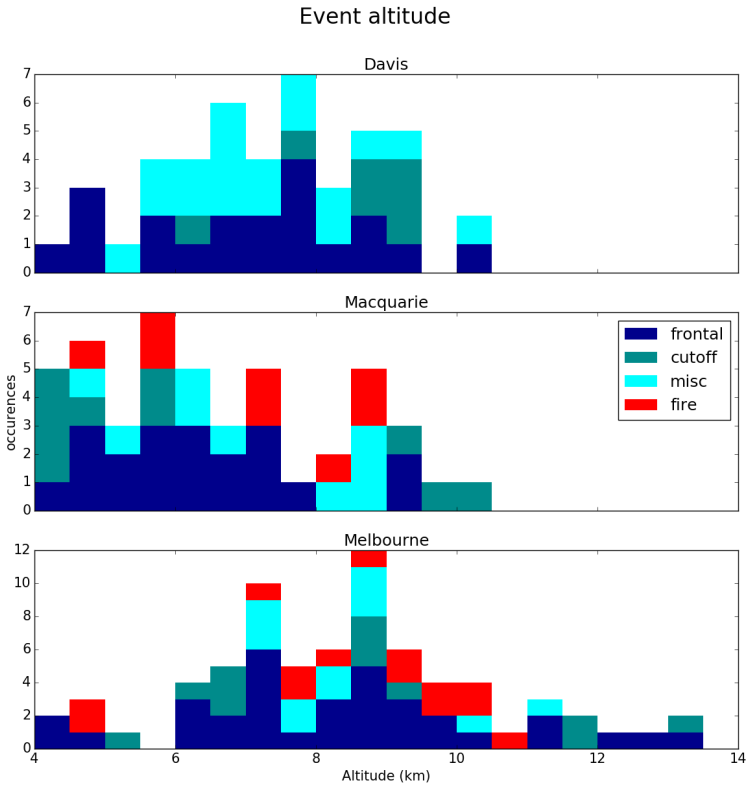

Figure 8: The distribution of the ozone peak altitude for Davis, Macquarie Island, and Melbourne. This shows the altitude of detected events, based on the tropospheric ozone enhancement peak. Events are categorised by likely causes, with possible smoke influenced events displayed in red.

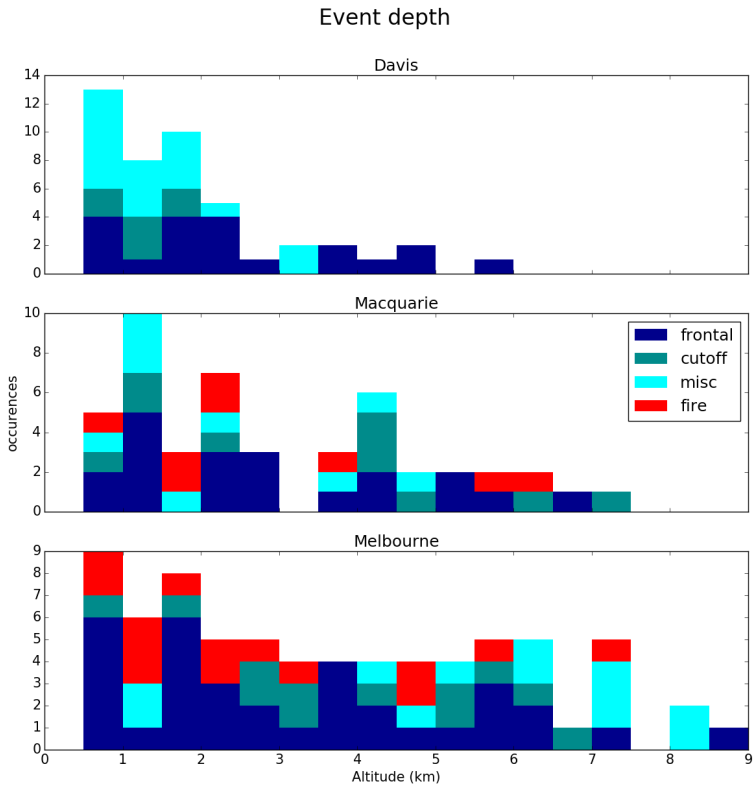

Figure 9: The distance between the ozone peak and the tropopause, and the cumulative probability of these distances (blue line) for Davis, Macquarie Island, and Melbourne. This shows the depth of the event into the troposphere, starting from the tropopause. The events filtered out as possibly smoke plume influenced are displayed here in red.

partial columns are checked, averaging seasonally for colocated data. Following this, an extrapolation is performed and the stratospherically sourced ozone is estimated over the latitude range from 35°S to 75°S. This range is used as it includes all three sites, a change of 5° in either direction at either end of the range changes the average tropospheric ozone by -8 to 9%. Examination of the GEOS-Chem output also gives us an insight as to whether the simulation can be used on its own in order to estimate STT event distribution and magnitude.

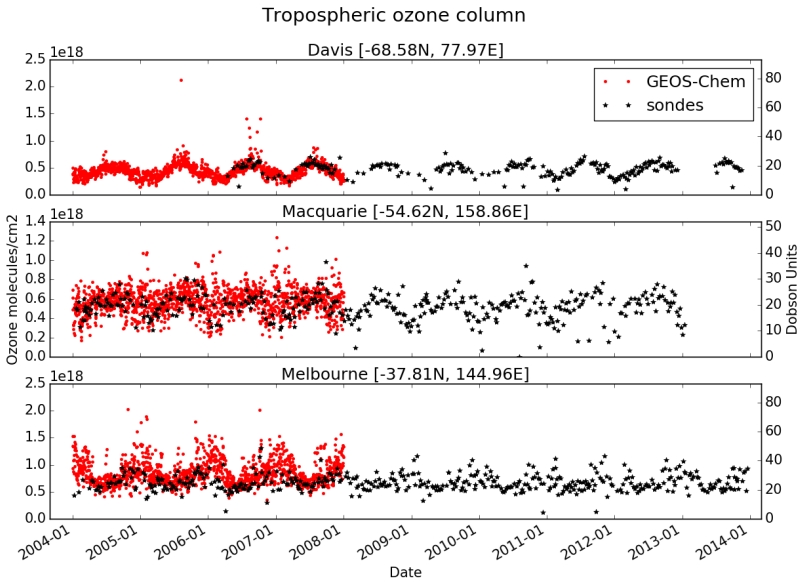

Figure 10: Tropospheric ozone column (Ω_{O3}, in molecules cm^{-2}) at daily resolution simulated by GEOS-Chem (red dots) from January 1 2004 to December 31 2013. The GEOS-Chem datapoints are respectively at 7AM, 11AM, and 11AM for Davis, Macquarie, and Melbourne. Columns calculated from ozonesondes are shown as black stars, each representing one measurement. (TODO: Update once fixed model run finishes)

Figure 10 compares the time series of tropospheric ozone column (Ω_{O_3}) in molecules cm^{-2} simulated by GEOS-Chem (red dots) to the measured tropospheric ozone columns (black stars). Sonde tropospheric columns are calculated using the GPH and ozone partial pressure recorded by the ozonesondes, using TODO: equation here. The seasonal cycles are well correlated, with similar timing and magnitude (paired r^2 values of TODO: run script when model run finished). The maximum ozone column at Melbourne occurs in summer, with a minimum in winter. Macquarie and Davis show the opposite seasonal cycle. The model shows more spread than the ozonesondes, although there are daily

simulated values for the model while only weekly or less for the ozonesondes.

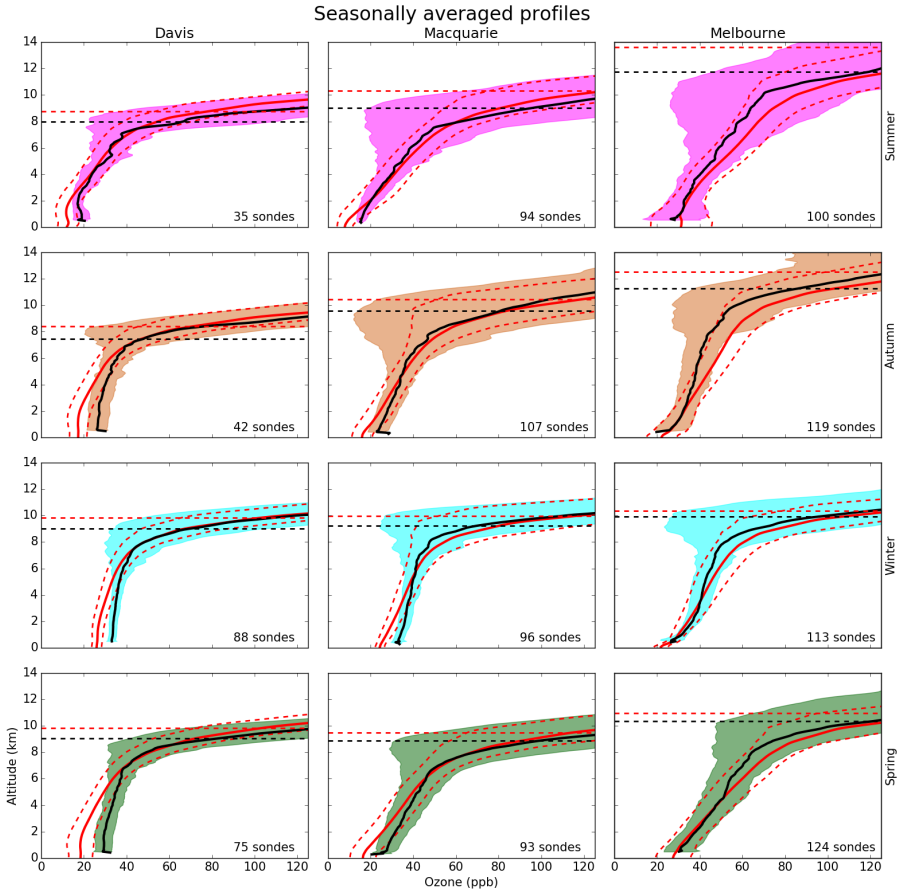

Figure 11: Tropospheric ozone (ppb) over Davis, Macquarie, and Melbourne, seasonally averaged. GEOS-Chem simulated data averaged over January 2005 until December 2013 are shown with red lines, with dashed red lines showing one standard deviation. Ozonesonde measurements are shown with black lines, and have seasonally coloured shaded areas over the mean plus or minus one standard deviation. Horizontal dotted line shows the mean tropopause heights, again red for the GEOS-Chem simulation and black for ozonesondes. TODO: Update once fixed model run finishes.

Figure 11 shows the measured and simulated seasonal mean ozone profile at all sites. The model generally underestimates ozone at low altitudes (up to 6 km) at both Davis and Macquarie, although this is less pronounced during summer. Over Melbourne an opposite bias is seen, where the model shows increased ozone levels from around 4 km up to the tropopause. Also notable is

the lower tropopause height exhibited by the model, which on average is lower by $\sim$ 1 km (TODO: mean bias, updated when model finishes). The effect of pollution and mainland influence can be seen over Melbourne, mostly during the summer months (DJF), as the lower altitudes have increased ozone mean as well as more variance

Although GEOS-Chem reasonably matches the ozonesonde tropospheric ozone column, it does not have the resolution required to capture STTs. Figure 12 shows the best (left) and worst (right) comparisons of ozone profiles up to 14 km between the ozonesondes and GEOS-Chem. The model output is shown in red, and is the average over 2° latitude by 2.5° longitude which contain the respective sonde release site. The vertical resolution from GEOS-Chem is too low to allow detection of STTs, with roughly 30 vertical levels up to the tropopause, while sondes have upwards of 100.

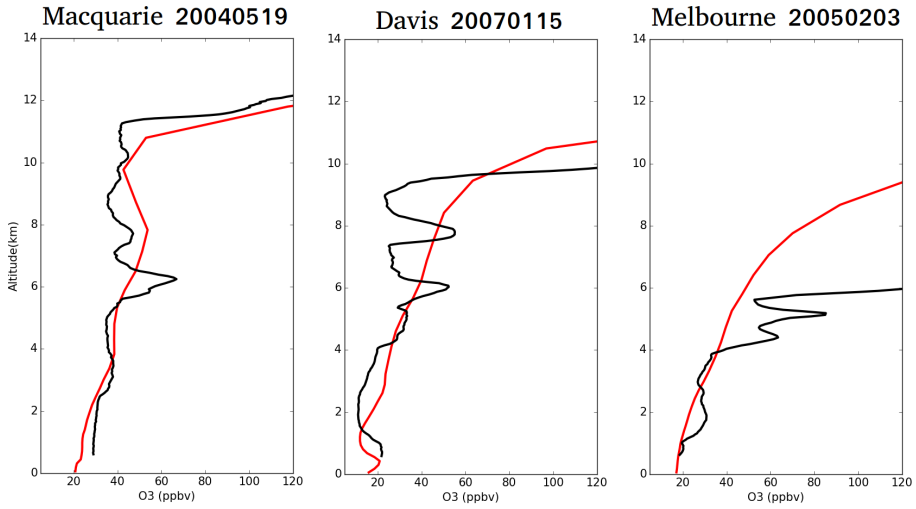

Figure 12: Ozonesonde profiles (black) against GEOS-Chem profiles (red) for three different dates, one over each site. The dates were picked based on subjective visual analysis as follows: left is the best match - May 19th 2004 over Macquarie, middle is an average case - January 15th, 2007 over Davis, and right is the worst match - February 3rd 2005 over Melbourne.

6 Stratosphere to troposphere ozone flux from STT events

Based on the integrated ozone amount associated with each STT event (see section 2.2), we find a lower bound for the STT ozone flux over each of our three sites (fire influence excluded). This is a conservative lower bound as the algo-

rithm ignores secondary ozone peaks which may also be transported down from the stratosphere, as well as ignoring potential ozone dispersion from the ozone peak. Figure 13 shows the mean fraction of total tropospheric column ozone attributed to stratospheric ozone intrusions at each site, averaged over days when an STT event occurs. The mean fraction of tropospheric ozone attributed to STT events is 2–4%, on individual days this value can exceed 10% at Macquarie and Melbourne. Figure 14 shows the data in absolute terms, and indicates that the mean STT event impact is around 1 to 2×10^{16} molecules/cm^2. Our flux estimates are relatively insensitive to our biomass burning filter; including smoke-influenced days changes the mean flux by less than 0.25% (5% relative change).

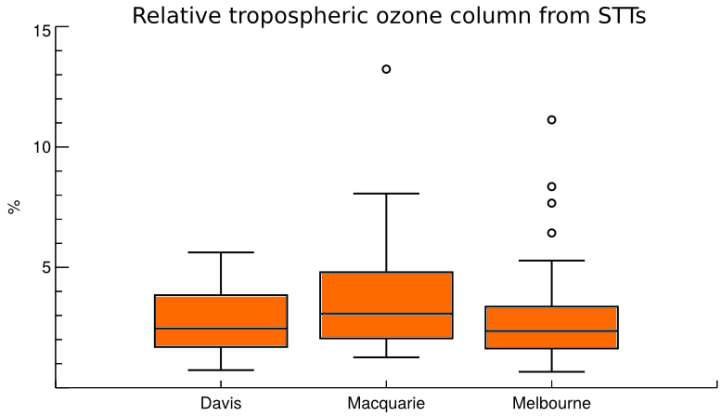

Figure 13: Fraction of total tropospheric column ozone attributed to stratospheric air intrusions during STT events.

Extrapolating out over the Southern Ocean using our estimated enhanced tropospheric ozone, we can create a rough estimate of the STT effect on tropospheric ozone in this region. This is be done by multiplying the monthly likelihoods of STTs with the monthly tropospheric column ozone amounts multiplied by our mean flux fraction. Taking the monthly likelihood from our ozonesonde events count per sondes released during each month, and southern latitude tropospheric column ozone amount from GEOS-Chem, the total amount of ozone from STT events over the southern ocean is at least (TODO:update once fixed model is finished) 2.2×10^{16} molecules cm^{-2} yr^{-1}, TODO: this is around X:TG/yr ozone. Figure 15 shows the seasonal STT contribution calculated this way, with 'l' and 'f' being the STT likelihood and fraction respectively.

Our estimate is (todo: greater/smaller/completely different) to other estimates of southern hemispheric ozone transport. Olsen [2003] use PV and winds from GEOS along with ozone measurements from TOMS to estimate that around 210 TG yr^{-1} of ozone flux occurs in 2000 between 30°S and 60°S.

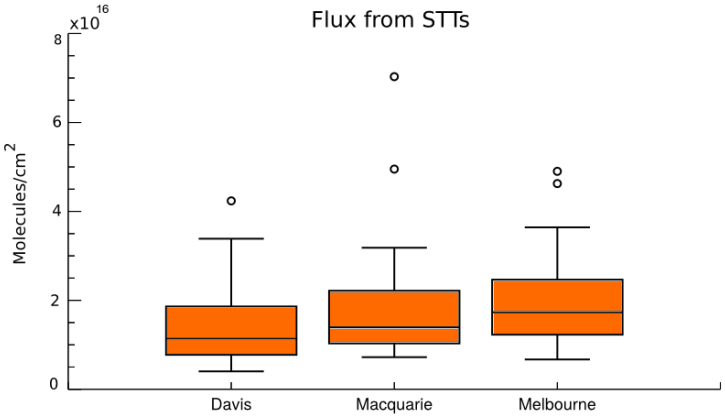

Figure 14: Tropospheric ozone attributed to stratospheric air intrusions during STT events.

Their estimates show a peak in flux from winter to early spring (JJAS), which is the same months when our GEOS-Chem simulation shows the highest tropospheric Ω_{O3}. Global STT flux estimated from an ensemble of models shows global STT flux at around 550 Tg yr^{-1} [Stevenson et al., 2006]. Global net flux (transport from the stratosphere to the troposphere minus opposite transport) is estimated to be 75 Tg yr^{-1} [Sprenger et al., 2003].

Considering the individual event contributions, Terao et al. [2008] estimate much higher STT impacts; where 30–40% of the tropospheric column is due to STT. Although this figure is based on the northern hemisphere during the seasonal STT peak.

7 Conclusions

Ozonesonde data in the Southern Hemisphere provides a satellite-independant quantification of STT ozone transport. The frequency and amount of ozone descending from the stratosphere into the troposphere can be estimated from the long time series of tropospheric ozone profiles. Using almost ten years of ozonesonde profiles over the southern high latitudes, a clear summer peak is seen for STT occurences at both 38°S and 55°S, although not at 69°S.

We use a Fourier bandpass filter to determine STT ozone transport events. The filter removes seasonal tropospheric ozone influences and allows clear detection of ozone-enhanced tongues of air in the troposphere. By setting empirical checks, ozonesonde vertical profiles can clearly show tropospheric ozone enhancement which is separated from the stratosphere. The cause of these ozone enhancements is examined through the use of satellite and reanalysis datasets on case studies above Melbourne. The major causes of STT events found over

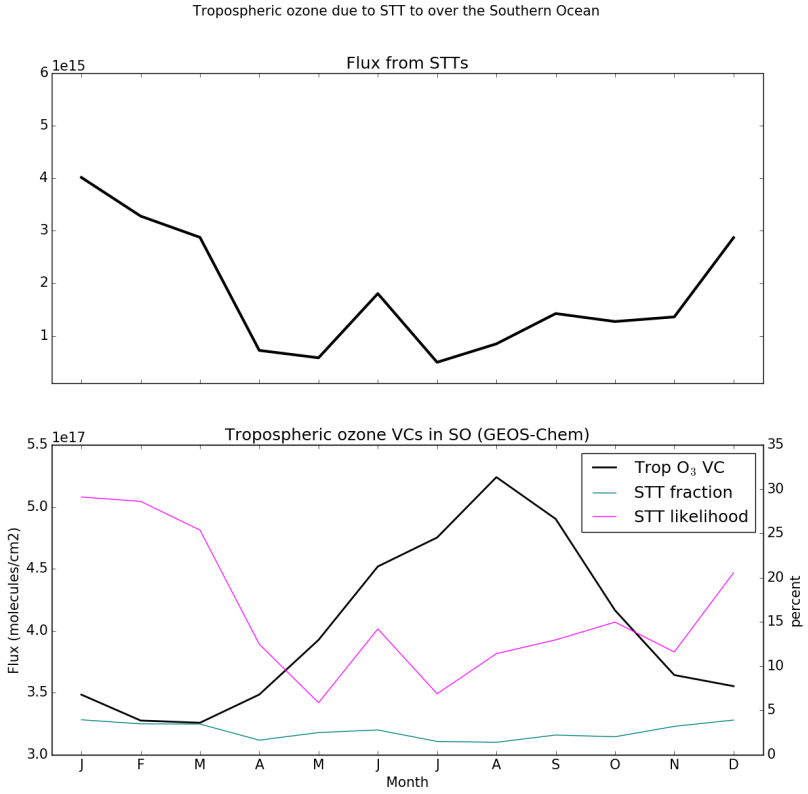

Figure 15: Top panel shows the estimated STT contribution to tropospheric ozone VC. Bottom panel shows the three factors multiplied together in order to produce the estimation. Units for 'l' and 'f' are on the right, while units for ozone VC amounts are on the left.

Melbourne are turbulent weather in the upper troposphere due to low pressure fronts and cut-off low pressure systems.

Integration of the ozone enhancement along the altitude of the ozone profile allows a rough estimate of stratospheric transport for each event. Events typically cause a 3% enhancement of the tropospheric ozone column. This is around 2×10^{15} molecules cm^{-2} (TODO: Update when model run finishes) ozone enhancement over the southern high latitudes caused by STTs.

GEOS-Chem performs fairly well when compared to ozonesondes at our three sites, with vertical profile averages and seasonal cycles of tropospheric ozone conforming to within $\sim 10\%$ (TODO: update when model finishes) of the data, even though the model is looking at the average over 2° latitude by 2.5° longitude grid boxes.

References

AIRS3STD, 2013.

S. P. Alexander, D. J. Murphy, and A. R. Klekociuk. High resolution VHF radar measurements of tropopause structure and variability at Davis, Antarctica (69?? S, 78?? E). *Atmospheric Chemistry and Physics*, 13(6):3121–3132, 2013. ISSN 16807324. doi: 10.5194/acp-13-3121-2013. URL `http://www.atmos-chem-phys.net/13/3121/2013/`.

Shiri Avnery, Denise L. Mauzerall, Junfeng Liu, and Larry W. Horowitz. Global crop yield reductions due to surface ozone exposure: 2. Year 2030 potential crop production losses and economic damage under two scenarios of O 3 pollution. *Atmospheric Environment*, 71(13):408–409, 2013. ISSN 13522310. doi: 10.1016/j.atmosenv.2012.12.045. URL `http://dx.doi.org/10.1016/j.atmosenv.2011.01.002`.

J. L. Baray, V. Daniel, G. Ancellet, and B. Legras. Planetary-scale tropopause folds in the southern subtropics. *Geophysical Research Letters*, 27(3):353–356, 2000. ISSN 00948276. doi: 10.1029/1999GL010788.

M. Beekmann, G. Ancellet, S. Blonsky, D. De Muer, A. Ebel, H. Elbern, J. Hendricks, J. Kowol, C. Mancier, R. Sladkovic, H. G J Smit, P. Speth, T. Trickl, and Ph Van Haver. Regional and global tropopause fold occurrence and related ozone flux across the tropopause. *Journal of Atmospheric Chemistry*, 28(1-3):29–44, 1997. ISSN 01677764. doi: 10.1023/A:1005897314623.

S. Bethan, G. Vaughan, and S. J. Reid. A comparison of ozone and thermal tropopause heights and the impact of tropopause definition on quantifying the ozone content of the troposphere. *Quarterly Journal of the Royal Meteorological Society*, 122(532):929–944, 1996. ISSN 00359009. doi: 10.1002/qj.49712253207. URL `http://doi.wiley.com/10.1002/qj.49712253207`.

Isabelle Bey, Daniel J. Jacob, Robert M. Yantosca, Jennifer A. Logan, Brendan D. Field, Arlene M. Fiore, Qin-Bin Li, Hong-Yu Liu, Loretta J. Mickley, and Martin G. Schultz. Global Modeling of Tropospheric Chemistry with Assimilated Meteorology: Model Description and Evaluation. *Journal of Geophysical Research*, 106:73–95, 2001. ISSN 0148-0227. doi: 10.1029/2001JD000807.

Edwin F. Danielsen. Stratospheric-Tropospheric Exchange Based on Radioactivity, Ozone and Potential Vorticity, 1968. ISSN 0022-4928.

S S Das, M V Ratnam, K N Uma, K V Subrahmanyam, and I A Girach. Influence of tropical cyclones on tropospheric ozone : possible implication. *Atmospheric Chemistry and Physics (Discussions)*, 15(2003):19305–19323, 2016. ISSN 1680-7324. doi: 10.5194/acpd-15-19305-2015.

D P Dee, S M Uppala, A J Simmons, P Berrisford, P Poli, S Kobayashi, U Andrae, M A Balmaseda, G Balsamo, P Bauer, P Bechtold, A C M Beljaars, L van de Berg, J Bidlot, N Bormann, C Delsol, R Dragani, M Fuentes, A J Geer, L Haimberger, S B Healy, H Hersbach, E V HÃ³lm, L Isaksen, P KÃ¥llberg, M KÃ¶hler, M Matricardi, A P McNally, B M Monge-Sanz, J.-J. Morcrette, B.-K. Park, C Peubey, P de Rosnay, C Tavolato, J.-N. ThÃ©paut, and F Vitart. The ERA-Interim reanalysis: configuration and performance of the data assimilation system. *Quarterly Journal of the Royal Meteorological Society*, 137(656):553–597, 2011. ISSN 1477-870X. doi: 10.1002/qj.828. URL `http://dx.doi.org/10.1002/qj.828`.

Sebastian D. Eastham, Debra K. Weisenstein, and Steven R H Barrett. Development and evaluation of the unified tropospheric-stratospheric chemistry extension (UCX) for the global chemistry-transport model GEOS-Chem. *Atmospheric Environment*, 89:52–63, 2014. ISSN 13522310. doi: 10.1016/j.atmosenv.2014.02.001. URL `http://dx.doi.org/10.1016/j.atmosenv.2014.02.001`.

D. P. Edwards. Tropospheric ozone over the tropical Atlantic: A satellite perspective. *Journal of Geophysical Research*, 108(D8):4237, 2003. ISSN 0148-0227. doi: 10.1029/2002JD002927. URL `http://doi.wiley.com/10.1029/2002JD002927`.

D. P. Edwards, L. K. Emmons, J. C. Gille, A. Chu, J. L. Attié, L. Giglio, S. W. Wood, Jim Haywood, M. N. Deeter, S. T. Massie, D. C. Ziskin, and James R. Drummond. Satellite-observed pollution from Southern Hemisphere biomass burning. *Journal of Geophysical Research Atmospheres*, 111(14):1–17, 2006. ISSN 01480227. doi: 10.1029/2005JD006655.

P. Forster, V. Ramaswamy, P. Artaxo, T. Berntsen, R. Betts, D.W. Fahey, J. Haywood, J. Lean, D.C. Lowe, G. Myhre, J. Nganga, R. Prinn, G. Raga, M. Schulz, and R. Van Dorland. Changes in Atmospheric Constituents and in Radiative Forcing. In: Climate Change 2007: The Physical Science Basis.

Contribution of Working Group I to the Fourth Assessment Report of the Intergovernmental Panel on Climate Change[Solomon, S., D. Qin, M. Man, 2007. URL https://www.ipcc.ch/publications_and_data/ar4/wg1/en/ch2.html.

W. Frey, R. Schofield, P. Hoor, D. Kunkel, F. Ravegnani, a. Ulanovsky, S. Viciani, F. D'Amato, and T. P. Lane. The impact of overshooting deep convection on local transport and mixing in the tropical upper troposphere/lower stratosphere (UTLS). *Atmospheric Chemistry and Physics*, 15 (11):6467–6486, 2015. ISSN 1680-7324. doi: 10.5194/acp-15-6467-2015. URL http://www.atmos-chem-phys.net/15/6467/2015/.

E. Galani. Observations of stratosphere-to-troposphere transport events over the eastern Mediterranean using a ground-based lidar system. *Journal of Geophysical Research*, 108(D12):1–10, 2003. ISSN 0148-0227. doi: 10.1029/2002JD002596. URL http://www.agu.org/pubs/crossref/2003/2002JD002596.shtml.

A. B. Guenther, X. Jiang, C. L. Heald, T. Sakulyanontvittaya, T. Duhl, L. K. Emmons, and X. Wang. The model of emissions of gases and aerosols from nature version 2.1 (MEGAN2.1): An extended and updated framework for modeling biogenic emissions. *Geoscientific Model Development*, 5(6):1471–1492, 2012. ISSN 1991959X. doi: 10.5194/gmd-5-1471-2012.

Ben Henderson. TOMS OH Fix, 2016. URL http://wiki.seas.harvard.edu/geos-chem/index.php/FAST-JX_v7.0_photolysis_mechanism#Fix_for_TOMS_to_address_strange_cycle_in_OH_output.

M C Jacobson and H Hansson. Organic atmospheric aerosols: Review and state of the science. *Reviews of Geophysics*, (38):267–294, 2000. ISSN 87551209. doi: 10.1029/1998RG000045.

Daniel a. Jaffe and Nicole L. Wigder. Ozone production from wildfires: A critical review. *Atmospheric Environment*, 51:1–10, 2012. ISSN 13522310. doi: 10.1016/j.atmosenv.2011.11.063. URL http://dx.doi.org/10.1016/j.atmosenv.2011.11.063.

A. O. Langford, J. Brioude, O. R. Cooper, C. J. Senff, R. J. Alvarez, R. M. Hardesty, B. J. Johnson, and S. J. Oltmans. Stratospheric influence on surface ozone in the Los Angeles area during late spring and early summer of 2010. *Journal of Geophysical Research Atmospheres*, 117(3):1–17, 2012. ISSN 01480227. doi: 10.1029/2011JD016766.

Allen S. Lefohn, Heini Wernli, Douglas Shadwick, Sebastian Limbach, Samuel J. Oltmans, and Melvyn Shapiro. The importance of stratospheric-tropospheric transport in affecting surface ozone concentrations in the western and northern tier of the United States. *Atmospheric Environment*, 45(28):4845–4857, 2011. ISSN 13522310. doi: 10.1016/j.atmosenv.2011.06.014. URL http://dx.doi.org/10.1016/j.atmosenv.2011.06.014.

Meiyun Lin, Arlene M. Fiore, Owen R. Cooper, Larry W. Horowitz, Andrew O. Langford, Hiram Levy, Bryan J. Johnson, Vaishali Naik, Samuel J. Oltmans, and Christoph J. Senff. Springtime high surface ozone events over the western United States: Quantifying the role of stratospheric intrusions. *Journal of Geophysical Research Atmospheres*, 117(19):1–20, 2012. ISSN 01480227. doi: 10.1029/2012JD018151.

C H Mari, G Cailley, L Corre, M Saunois, Atti´ E, J L, V Thouret, and A Stohl. Tracing biomass burning plumes from the Southern Hemisphere during the AMMA 2006 wet season experiment, Atmos. *Atmospheric Chemistry and Physics*, 8:3951–3961, 2008. ISSN 1680-7324. doi: 10.5194/acpd-7-17339-2007.

M Mihalikova, S Kirkwood, J Arnault, and D Mikhaylova. Observation of a tropopause fold by MARA VHF wind-profiler radar and ozonesonde at Wasa, Antarctica: comparison with ECMWF analysis and a WRF model simulation. *Annales Geophysicae*, 30(9):1411–1421, 2012. doi: 10.5194/angeo-30-1411-2012. URL `http://www.ann-geophys.net/30/1411/2012/`.

NOAA. NOAA Ozone sondes appendix. URL `http://www.ndsc.ncep.noaa.gov/organize/protocols/appendix5/`.

Mark a. Olsen. A comparison of Northern and Southern Hemisphere cross-tropopause ozone flux. *Geophysical Research Letters*, 30(7):1412, 2003. ISSN 0094-8276. doi: 10.1029/2002GL016538. URL `http://doi.wiley.com/10.1029/2002GL016538`.

B.C.a Pak, R.L.b Langenfelds, S.A.b Young, R.J.b Francey, C.P.b Meyer, L.M.b Kivlighon, L.N.b Cooper, B.Lb Dunse, C.E.b Allison, L.P.b Steele, IE.b Galbally, and I.A.b Weeks. Measurements of biomass burning influences in the troposphere over southeast Australia during the SAFARI 2000 dry season campaign. *Journal of Geophysical Research D: Atmospheres*, 108(13):SAF 16–1 – SAF 16–10, 2003. ISSN 0148-0227. doi: 10.1029/2002JD002343. URL `http://www.scopus.com/inward/record.url?eid=2-s2.0-0742322536&partnerID=40&md5=cafaeef03b948fb456696583ed3ab9a5`.

J. D. Price and G. Vaughan. The potential for stratosphere-troposphere exchange in cut-off-low systems. *Quarterly Journal of the Royal Meteorological Society*, 119(510):343–365, 1993. doi: 10.1002/qj.49711951007. URL `http://onlinelibrary.wiley.com/doi/10.1002/qj.49711951007/abstract`.

P. Reutter, B. Škerlak, M. Sprenger, and H. Wernli. Stratosphere-troposphere exchange (STE) in the vicinity of North Atlantic cyclones. *Atmospheric Chemistry and Physics*, 15(19):10939–10953, 2015. ISSN 16807324. doi: 10.5194/acp-15-10939-2015.

N E Selin, S Wu, K M Nam, J M Reilly, S Paltsev, R G Prinn, and M D Webster. Global health and economic impacts of future ozone pollution.

Environmental Research Letters, 4(4):044014, 2009. ISSN 1748-9326. doi: 10.1088/1748-9326/4/4/044014.

Parikhit Sinha, Lyatt Jaeglé, Peter V. Hobbs, and Qing Liang. Transport of biomass burning emissions from southern Africa. *Journal of Geophysical Research*, 109:D20204, 2004. ISSN 01480227. doi: 10.1029/2004JD005044.

Herman G J Smit, Wolfgang Straeter, Bryan J. Johnson, Samuel J. Oltmans, Jonathan Davies, David W. Tarasick, Bruno Hoegger, Rene Stubi, Francis J. Schmidlin, T. Northam, Anne M. Thompson, Jacquelyn C. Witte, Ian Boyd, and Françoise Posny. Assessment of the performance of ECC-ozonesondes under quasi-flight conditions in the environmental simulation chamber: Insights from the Juelich Ozone Sonde Intercomparison Experiment (JOSIE). *Journal of Geophysical Research Atmospheres*, 112(19):1–18, 2007. ISSN 01480227. doi: 10.1029/2006JD007308.

Michael Sprenger, Mischa Croci Maspoli, and Heini Wernli. Tropopause folds and cross-tropopause exchange: A global investigation based upon ECMWF analyses for the time period March 2000 to February 2001. *Journal of Geophysical Research: Atmospheres*, 108(D12):n/a—-n/a, 2003. ISSN 2156-2202. doi: 10.1029/2002JD002587. URL `http://dx.doi.org/10.1029/2002JD002587`.

D S Stevenson, F J Dentener, M G Schultz, K Ellingsen, T P C van Noije, O Wild, G Zeng, M Amann, C S Atherton, N Bell, D J Bergmann, I Bey, T Butler, J Cofala, W J Collins, R G Derwent, R M Doherty, J Drevet, H J Eskes, A M Fiore, M Gauss, D A Hauglustaine, L W Horowitz, I S A Isaksen, M C Krol, J.-F. Lamarque, M G Lawrence, V Montanaro, J.-F. Müller, G Pitari, M J Prather, J A Pyle, S Rast, J M Rodriguez, M G Sanderson, N H Savage, D T Shindell, S E Strahan, K Sudo, and S Szopa. Multimodel ensemble simulations of present-day and near-future tropospheric ozone. *J. Geophys. Res.*, 111(D8), 2006. doi: 10.1029/2005jd006338. URL `http://dx.doi.org/10.1029/2005JD006338`.

Andreas Stohl, Heini Wernli, Paul James, Michel Bourqui, Caroline Forster, Mark A. Liniger, Petra Seibert, and Michael Sprenger. A new perspective of stratosphere-troposphere exchange. *Bulletin of the American Meteorological Society*, 84(11):1565–1573+1473, 2003. ISSN 00030007. doi: 10.1175/BAMS-84-11-1565.

Q. Tang and M. J. Prather. Correlating tropospheric column ozone with tropopause folds: The Aura-OMI satellite data. *Atmospheric Chemistry and Physics*, 10(19):9681–9688, 2010. ISSN 16807316. doi: 10.5194/acp-10-9681-2010.

Q. Tang and M. J. Prather. Five blind men and an elephant: can NASA Aura measurements quantify the stratosphere-troposphere exchange of ozone flux? *Atmospheric Chemistry and Physics*, 11(5):2357–2380, 2012. ISSN

16807316. doi: 10.5194/acp-12-2357-2012. URL http://dx.doi.org/10.5194/acpd-11-26897-2011.

Yukio Terao, Jennifer A Logan, Anne R Douglass, and Richard S Stolarski. Contribution of stratospheric ozone to the interannual variability of tropospheric ozone in the northern extratropics. *J. Geophys. Res.*, 113(D18), 2008. doi: 10.1029/2008jd009854. URL http://dx.doi.org/10.1029/2008jd009854.

Yoshihiro Tomikawa, Yashiro Nishimura, and Takashi Yamanouchi. Characteristics of Tropopause and Tropopause Inversion Layer in the Polar Region. *SOLA*, 5:141–144, 2009. doi: 10.2151/sola.2009-036. URL http://dx.doi.org/10.2151/sola.2009-036.

G Vaughan, J D Price, and A Howells. Transport into the troposphere in a tropopause fold. *Quarterly Journal of the Royal Meteorological Society*, 120 (518):1085–1103, 1993. ISSN 00359009. doi: 10.1002/qj.49712051814.

Volkmar Wirth. Diabatic heating in an axisymmetric cut-off cyclone and related stratosphere-troposphere exchange. *Quarterly Journal of the Royal Meteorological Society*, 121(521):127–147, 1995. ISSN 00359009. doi: 10.1002/qj.49712152107. URL http://doi.wiley.com/10.1002/qj.49712152107.

World Meteorological Organization WMO. Meteorology A Three-Dimensional Science. *Geneva, Second Session of the Commission for Aerology*, 4:134–138, 1957.

L Zhang, D J Jacob, X Yue, N V Downey, D A Wood, and D Blewitt. Sources contributing to background surface ozone in the US Intermountain West. *Atmos. Chem. Phys.*, 14(11):5295–5309, 2014. doi: 10.5194/acp-14-5295-2014. URL http://dx.doi.org/10.5194/acp-14-5295-2014.